Microstructural and heat transfer modeling of selective laser melting in austenitic stainless steels

M.P. Sotiriou[1], J.S. Aristeidakis[1], S.A. Koimtzidis[1], I. Papadioti[1], M.I.T. Tzini[2], G.N. Haidemenopoulos[1] and N. Aravas[1,3]

[1]*Department of Mechanical Engineering, University of Thessaly, Pedion Areos, 38334 Volos, Greece*
[2]*Department of Materials Science and Engineering, Massachusetts Institute of Technology, 77 Massachusetts Ave. 02139 Cambridge, MA, USA*
[3]*International Institute for Carbon Neutral Research (WPI-I2CNER), Kyushu University, 774 Motooka, Nishi-ku, Fukuoka 819-0395, Japan*

Abstract

In this study, a thermal analysis coupled with microstructural evolution models is used to simulate Selective Laser Melting (SLM) in austenitic stainless steels. CALPHAD-based modeling is applied to predict non-equilibrium thermophysical properties under rapid cooling conditions. Heat transfer and diffusion analyses are carried out in sequence. Thermal simulations are performed using FEM, considering the effect of the powder. The calculated temperature history is provided as input for the microstructural simulation of solidification and solid-state transformations. The methodology is applied on an AISI 316L austenitic stainless steel as a case study to establish a benchmark simulation scheme for SLM and other Additive Manufacturing (AM) processes.

1. INTRODUCTION

Selective laser melting was simulated following an integrated methodology that involved heat transfer calculations coupled with microstructural evolution models to capture the microstructural evolution of an AISI 316L stainless steel specimen. A rapid cooling model was developed to predict the material's thermophysical properties, both in consolidated state and powder form. Heat transfer and diffusion analyses are then employed in sequence. The aforementioned properties were provided for a 2D heat transfer analysis, carried out throughout the building process, in order to calculate the development of spatial and temporal temperature distribution. The final temperature results were utilized by diffusion models to predict the resulting microstructural characteristics. Although the analysis addresses a 316L system, similar microstructural modeling can be applied for the vast majority of austenitic stainless steels that solidify with single austenite under the severe non-equilibrium conditions that develop in SLM.

2. METHODOLOGY

Simulation concerned a benchmark 316L system with composition given in *Table 1*, under the manufacturing conditions described in 2D SLM experiments conducted by Bertsch et al. [1]. A schematic

illustration of the applied methodology, including a final mechanical analysis that is not elaborated upon the present study, is given in *Figure 1*.

Table 1: *AISI 316L composition in wt%*

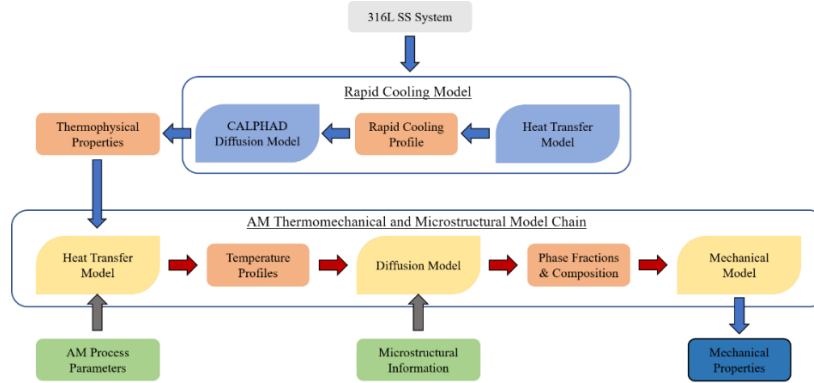| 316L	Cr	Ni	Mo	C	Mn	Fe
Composition (wt%)	18.39	13.94	2.6	0.03	1.47	bal.

Figure 1: *Flowchart of the proposed simulation methodology for additive manufacturing processes.*

2.1 Rapid cooling and diffusion models

Accurate simulation of the transient heat transfer in selective laser melting required development of a rapid cooling model to calculate temperature-dependent non equilibrium thermophysical properties. CALPHAD-based microstructural evolution models were employed to simulate solidification and subsequent solid-state transformations upon the applied temperature gradients. A prototype cooling path was considered, as calculated in [2] to act as a first-degree approximation of the actual cooling behavior. Multi-component and multi-phase, one-dimensional mass transfer calculations were performed in the DICTRA module of Thermo-Calc [3], utilizing thermodynamic and mobility information provided in the TCFE11 and MOBFE2 databases respectively.

A planar geometry cell with 0.5 μm length was considered as a representative elementary structure, accounting for the transverse evolution of the primary dendrites (columns) that constitute the dominant microstructural feature. Initially, the cell was comprised of a single liquid region. In contrast with previous attempts to describe the behavior of AISI 316L [2,4], austenite was considered to be the single solidifying phase, ignoring the effect of ferrite in eutectic or peritectic solidification. Thus, an inactive γ-austenite region was modeled adjacent to the liquid and separated by a moving interface. The reasoning behind omitting δ-ferrite from the simulation is that under extreme cooling rates, dendritic epitaxial growth regulates the microstructural evolution and promotes exclusive austenite (stable in a lower temperature range) growth through elevated solidification velocities. The nucleation stage is omitted from the analysis since only diffusion-controlled transformations are considered in DICTRA.

Non-equilibrium thermophysical properties were predicted for a temperature range spanning from 27°C to 2500°C based on the calculated phase fractions and compositions from the DICTRA

simulations using the first-degree approximation of the cooling curve. Density ρ, specific heat capacity c_p and latent heat U_L were computed directly from Thermo-Calc, for the non-equilibrium segregation profiles during cooling and then the transient thermophysical properties were calculated as a function of temperature by means of integration over the diffusion cell domains. The latent heat was determined after numerical integration of its first temperature derivative that was calculated from changes in enthalpy. Finally, for the thermal conductivity k, additional experimental data [5] were incorporated in the analysis since the employed databases lack information regarding conductivity. Notice that the diffusion model was formulated under the same principles, but considered the complete temperature history profiles that were calculated. The results were obtained in terms of terminal phase fractions and constitutions.

2.2 Heat transfer model

The heat transfer modeling applied by Sotiriou et al. [2] was implemented as the theoretical basis for the present simulation, using ABAQUS, a general-purpose finite element software [6]. Aiming to provide a sophisticated formulation to better describe SLM conditions, the effect of the deposited powder on top of the built material, as well as of the powder surrounding the built specimen, was considered. An enhancement in the quite element method [7] involved the consideration of powder as an intermediate state of "activated" material points, representing metal deposition regions. between the initial ($k=0$ and $c_p=0$) and the terminal ($k=k_s$ and $c_p=c_{p,s}$), where index s stands for the post-solidification material. This intermediate state would exhibit the effective thermophysical properties of AISI 316L powder, calculated as that were those of the solid materials multiplied with the atomic packing factor (APF=0.74 for powder stacking roughly in close-structure FCC under the effect of gravity). An important exception is the thermal conductivity, where an in-depth modeling approach was followed. Considering the resultant heat transfer flux that comprises of conduction-radiation components acting among the powder grains, an equivalent temperature-time-dependent conduction factor k_p was formulated according to de Moraes and Czekanski [8] and is given in *Figure 2a*.

Simulation of the building process of a 1.5x1.5 *mm* 2D rectangular wall was carried out, following a unidirectional scanning strategy (right to left) and a fine meshing to capture the rapid heating phenomena. Laser velocity was taken equal to $u=675$ *mm/s*, power $P=100$ *W,* layer thickness 0.02 *mm*, chamber temperature $T_\infty=27°C$ and idle time 10 *s* between consecutive passes. A single-ellipsoid volumetric source was employed to formulate the heat input by the moving laser beam ($a=40$ *μm*, $c=20$ *μm*, $b=1$ *mm* accounting for the 2D analysis). Applied boundary conditions consisted of convection-radiation for the areas in contact with the atmosphere and conduction-radiation (in equivalent conduction terms) for all powder-submerged free surface areas that were formulated by modifying the analytical solution for conduction in a semi-infinite medium. The substrate geometry was omitted since building in [1] employed construction of supporting columns that accounted for less than 5% of the total base area. Thus, a conduction-convection boundary condition was applied instead. Finally, anemometry and Marangoni effects were taken into account due to the effect of forced convection caused by the laser beam in surrounding atmosphere and the liquid metal respectively.

3. RESULTS AND DISCUSSION

3.1 Thermophysical properties

The calculated temperature-dependent thermophysical properties for the reference 316L system are given in *Figure 2*. Notice that both consolidated (black lines) and powder (red lines) properties are provided. Latent heat of solidification is calculated to be $U_L = 1976.65 \; kJ/kg$. An important remark concerns the difference in order of magnitude between powder and consolidated form materials.
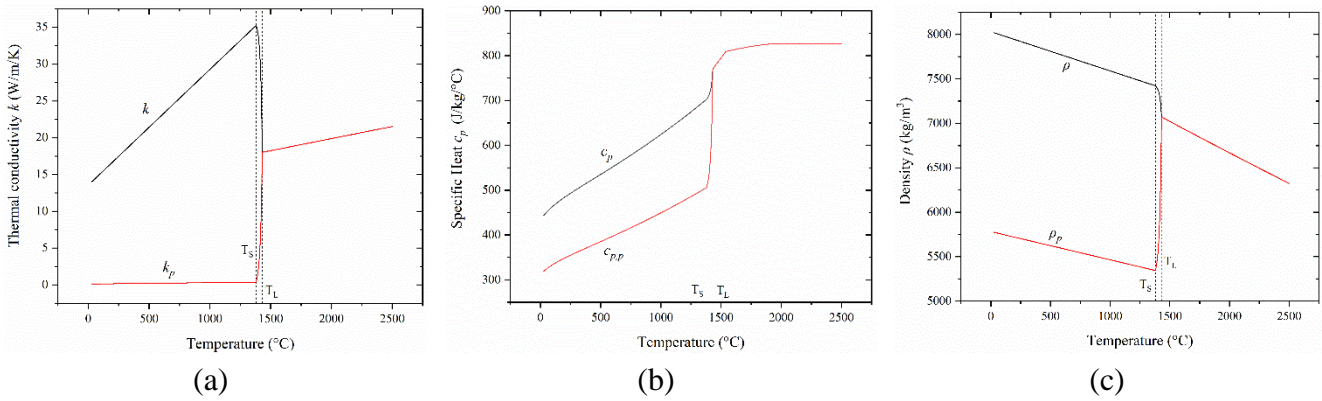

Figure 2: Thermophysical properties of consolidated (red lines) and powder (black lines) 316L: (a) Thermal conductivity k, (b) Specific heat capacity c_p and (c) Density ρ.

3.2 Temperature history and microstructural constitution

Temperature results for three middle material points at different built heights are presented in *Figure 3(a)*. Every material point is subjected to melting and rapid cooling followed by a thermal cycling behavior which culminates in slow cooling to ambient temperature after the end of the process. It is evident that under the given process parameters, each node melted and solidified twice, enabling joining of the deposited material with the previous layers. Initially, heat accumulation takes place upon subsequent laser passes, as the boundary conditions cannot remove heat efficiently, as indicated by the rise of the minimum thermal-cycle temperatures. However, after $520°C$ a linear decrease is noticed.
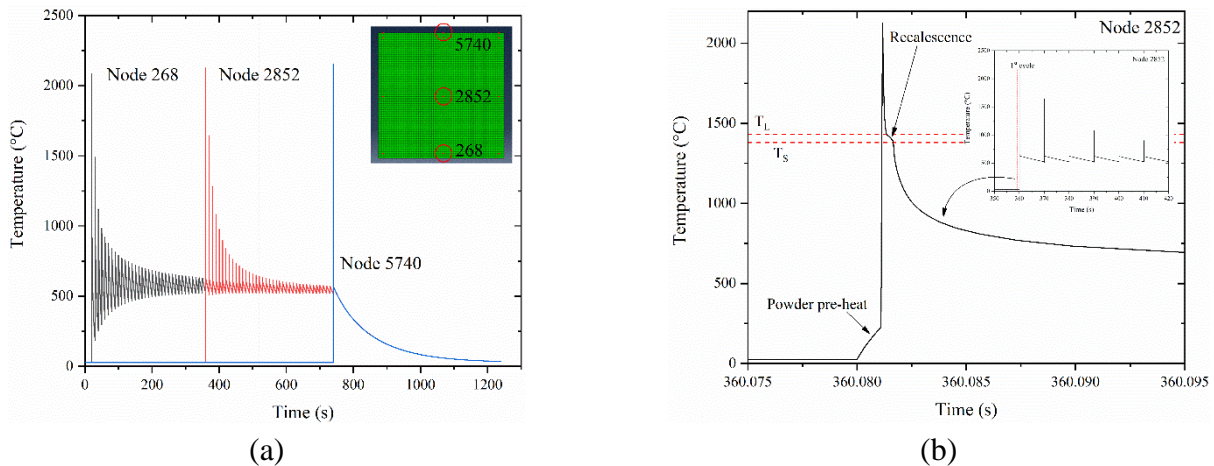

Figure 3: Temperature history results: (a) Spatial comparison and (b) first temperature cycle N2852

4

Modeling provided several insights as well, regarding short-lived and transient heat transfer phenomena taking place during printing. In *Figure 3(b)*, the first thermal cycle for central node 2852 is presented. Notice that ambient-temperature powder is subjected to pre-heating, due to heat influx from the previously built layer that has an elevated temperature. Recalescence -the effect of latent heat on the temperature profile- appears, controlling the cooling rate during solidification. Moreover, each cooling stage exhibits a change of rate, from rapid cooling initially, to controlled heat abduction towards the end. This is signified by conduction within the specimen, transferring heat more efficiently than free-surface areas can reject toward the environment. Evidently, the built wall becomes saturated in heat (no internal temperature gradients) and thus the total rate of cooling decreases. At this stage the temperature profiles of all material points coincide, as observed in *Figure 3(a)*.

The temperature profile of node 2852 was employed to calculate the microstructural evolution. Since the diffusion cell consists of austenite as the single solid phase, the solidification path in *Figure 4(a)* does not exhibit cyclic behavior as observed in δ-ferrite-containing systems [2]. However, a decrease in the solidus temperature at $1300.4°C$, leads to an increase of the freezing range by almost $70°C$ in comparison to the rapid cooling model, with the additional range covering less than *1%* of solidification. Interestingly, this behavior could not be simulated with the limit case of Scheil-Gulliver approach as described in [2], due to simulation termination criteria.
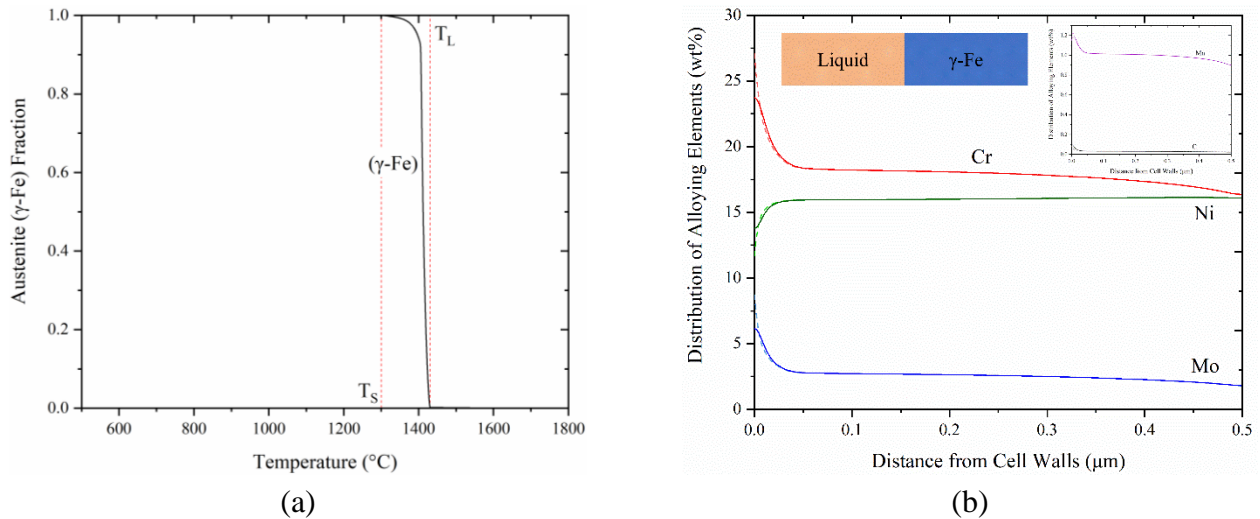

(a)   (b)

Figure 4: *Microstructural analysis results: (a) Austenite fraction evolution with respect to temperature and (b) alloying elements segregation profiles. Dashed lines correspond to post-solidification and full lines to end of process profiles.*

Finally, *Figure 4(b)* illustrates the evolution of microsegregation profiles after the solidification (dashed lines) and up to the end of the process (solid lines). Cr and Mo tend to transfer away from austenite and segregate to the dendrite walls, in accordance with [2,4]. A decrease in segregation is observed for all alloying elements as the effect of thermal cycling upon subsequent laser passes for the deposition of new layers. Chromium microsegregation results are similar to values provided by EDS

experimental information conducted in [1], 20-22 *wt%* Cr in a region near the cell wall and 17 *wt%* Cr towards the cell core. The resulting microstructural information together with the temperature history can be provided as input for a mechanical analysis in order to calculate the residual stress field as well as the terminal mechanical properties of as-built AISI 316L SLM products.

4. CONCLUSIONS

An integrated methodology of modeling and simulation of SLM in 316L austenitic stainless steel is established. Transient heat transfer analysis employed non-equilibrium thermophysical properties to calculate temperature profiles with high fidelity, taking into account the effect of material powder. The diffusion model determined the microstructural constitution in accordance with literature experimental results. The present analysis constitutes a benchmark SLM simulation methodology for austenitic stainless steels that solidify only with austenite.

5. REFERENCES

[1]   K.M. Bertsch, G. Meric de Bellefon, B. Kuehl, D.J. Thoma, Origin of dislocation structures in an additively manufactured austenitic stainless steel 316L, *Acta Mater. 199* (2020) 19–33. doi:10.1016/j.actamat.2020.07.063.

[2]   M.P. Sotiriou, J.S. Aristeidakis, M.-I.T. Tzini, I. Papadioti, G.N. Haidemenopoulos, N. Aravas, Microstructural and Thermomechanical Simulation of the Additive Manufacturing Process in 316L Austenitic Stainless Steel, *Mater. Proc.* 2021, *3*, 20. doi:10.3390/iec2m-09237.

[3]   J.-O. Andersson, T. Helander, L. Hoglund, P. Shi, B. Sundman, THERMO-CALC & DICTRA, Computational Tools For Materials Science. *Calphad* 2002, *26*, 273–312, doi:10.1016/0378-1119(90)90056-W.

[4]   M.P. Sotiriou, M.I.T. Tzini, J.S. Aristeidakis, G.N. Haidemenopoulos, I. Barsoum, A computational study of solidification during additive manufacturing of AISI 304 austenitic stainless steel, in *Proceedings of the 7th Pan-Hellenic Conference on Meatals and Materials*, Athens 11-13 December 2019, https://www.researchgate.net/publication/337948458.

[5]   C.S. Kim, *Thermophysical Properties of Stainless Steels*; Argonne, IL, USA, 1975, doi:10.2172/4152287.

[6]   H.D. Hibbitt, ABAQUS/EPGEN—A general purpose finite element code with emphasis on nonlinear applications. *Nucl. Eng. Des.* 1984, *77*, 271–297, doi:10.1016/0029-5493(84)90106-7.

[7]   P. Michaleris, Modeling metal deposition in heat transfer analyses of additive manufacturing processes, Finite Elements in Analysis and Design. 86 (2014) 51–60. doi:10.1016/j.finel.2014.04.003.

[8]   D.A. de Moraes, A. Czekanski, Parametric thermal fe analysis on the laser power input and powder effective thermal conductivity during selective laser melting of ss304l, *Journal of Manufacturing and Materials Processing*. 2 (2018). doi:10.3390/jmmp2030047.